

Mineralogy and olivine cooling rate of the Dhofar 019 shergottite

Takashi Mikouchi and Masamichi Miyamoto

*Department of Earth and Planetary Science, Graduate School of Science, University of Tokyo,
Hongo, Bunkyo-ku, Tokyo 113-0033*

Abstract: Dhofar 019 is a new basaltic shergottite found in Oman. It is mainly composed of pyroxenes, plagioclase glass, and olivine. Olivine grains show variable size distributions from large (~1 mm) non-euhedral zoned grains with magnesian cores (Fa₄₀) to small euhedral homogeneous grains with variable compositions (Fa₄₈₋₅₉). This may suggest that some of the Dhofar 019 olivines are xenocrysts and others are phenocrysts. The Dhofar 019 olivines are compositionally distinct from those in other shergottites. Pyroxenes are extensively zoned, and pigeonite cores are usually surrounded with augite rims, suggesting undercooling of magma to a similar degree as that of EETA79001 (lithology A) and Zagami. There appears to be a compositional change in major and minor elements from the magnesian pyroxenes to ferroan pyroxenes for both pigeonite and augite. The magnesian parts have similar compositions to EETA79001 (lithology A) pyroxenes, and the ferroan parts are similar to Zagami pyroxenes. Plagioclase zoning in Dhofar 019 more closely resembles that of Zagami. Spinel compositions in Dhofar 019 overlap those of EETA79001, and the Dhofar 019 chromite may be a xenocryst like EETA79001. The cooling rate of Dhofar 019 calculated from Fe-Mg zoning profiles of olivine is 0.05–0.1°C/hour. This corresponds to a burial depth of ~5 m from the martian surface, possibly in a lava flow. Thus, the groundmass crystallization of Dhofar 019 occurred near the martian surface, although it is likely that Dhofar 019 has experienced a complex history.

1. Introduction

With the recent discovery of several martian meteorites from the African deserts, the total number of martian meteorites is 19 (excluding paired samples) (Grossman and Zipfel, 2001). Most of these newly discovered specimens belong to basaltic shergottites, the largest group of martian meteorites (*e.g.*, McSween, 1994) (Table 1). However, the newly discovered samples are different in the respect that they contain olivine as major phases. The “classic” basaltic shergottites (Shergotty, Zagami, EETA79001 (lithology B), QUE94201, Los Angeles) are composed of pyroxene and plagioclase glass, and do not contain olivines (*e.g.*, McSween, 1994). These olivine-bearing basaltic shergottites are called “picritic” shergottites in some cases (Barrat *et al.*, 2002). Such picritic shergottites comprise two new groups of African meteorites. One group of five samples was found near Dar al Gani, Libya (Dar al Gani 476, 489, 735, 670, and 876) and the other group of four samples was found near Sayh al Uhaymir, Oman (Sayh al Uhaymir 005, 008, 051, and 094). Each group is believed to represent a single, separate fall (Folco and Franchi, 2000; Folco *et al.*, 2000; Zipfel, 2000; Zipfel *et al.*, 2000; Barrat *et al.*, 2001; Bartoschewitz and Ackermann, 2001; Hofmann *et al.*, 2001; Mikouchi *et al.*, 2001;

Table 1. Martian meteorites belonging to the "shergottite" group.

	Recovered location	Recovered year	Weight (kg)	Rock type	Major minerals
Shergotty	Shergahti, India	1865	~5	Basaltic	Pyroxenes, maskelynite
Zagami	Zagami, Nigeria	1962	~18	Basaltic	Pyroxenes, maskelynite
EETA79001 (lithology B)	Antarctica	1980	7.9*	Basaltic	Pyroxenes, maskelynite
QUE94201	Antarctica	1994	0.012	Basaltic	Pyroxenes, maskelynite
Los Angeles	California, USA	1999	0.70	Basaltic	Pyroxenes, maskelynite
Northwest Africa 480	Algeria?	2000	0.028	Basaltic	Pyroxenes, maskelynite
Northwest Africa 856	Morocco	2001	0.32	Basaltic	Pyroxenes, maskelynite
EETA79001 (lithology A)	Antarctica	1980	7.9*	Basaltic**	Pyroxenes, olivine, maskelynite
Dar al Gani 476 ^a	Libya	1998	2.01	Basaltic**	Pyroxenes, olivine, maskelynite
Dar al Gani 489 ^a	Libya	1997	2.15	Basaltic**	Pyroxenes, olivine, maskelynite
Dar al Gani 735 ^a	Libya	1996-97	0.59	Basaltic**	Pyroxenes, olivine, maskelynite
Dar al Gani 670 ^a	Libya	1998-99	1.62	Basaltic**	Pyroxenes, olivine, maskelynite
Dar al Gani 876 ^a	Libya	1998	0.006	Basaltic**	Pyroxenes, olivine, maskelynite
Sayh al Uhaymir 005 ^b	Sayh al Uhaymir, Oman	1999	1.34	Basaltic**	Pyroxenes, olivine, maskelynite
Sayh al Uhaymir 008 ^b	Sayh al Uhaymir, Oman	1999	8.58	Basaltic**	Pyroxenes, olivine, maskelynite
Sayh al Uhaymir 051 ^b	Sayh al Uhaymir, Oman	2000	0.44	Basaltic**	Pyroxenes, olivine, maskelynite
Sayh al Uhaymir 094 ^b	Sayh al Uhaymir, Oman	2001	0.23	Basaltic**	Pyroxenes, olivine, maskelynite
Dhofar 019	Dhofar, Oman	2000	1.06	Basaltic**	Pyroxenes, olivine, maskelynite
ALH-77005	Antarctica	1977	0.48	Lherzolitic	Olivine, pyroxenes, maskelynite
LEW88516	Antarctica	1988	0.013	Lherzolitic	Olivine, pyroxenes, maskelynite
Yamato-793605	Antarctica	1979	0.016	Lherzolitic	Olivine, pyroxenes, maskelynite

^{a,b} Five Dar al Gani and four Sayh al Uhaymir samples are possibly paired, respectively.

*Total mass of EETA79001. **Or "picritic"

Wadhwa *et al.*, 2001). Although they were discovered in Libya and Oman, respectively, their apparent similarities suggest that they have originated from the same igneous body on Mars and fell on the earth separately (*e.g.*, Zipfel, 2000; Nishiizumi *et al.*, 2001). The origins of olivine megacrysts in Dar al Gani/Sayh al Uhaymir shergottites are under dispute. They could be either “phenocrysts” that crystallized with the groundmass from the same magma or “xenocrysts” that are unrelated to the groundmass melt (*e.g.*, Folco *et al.*, 2000; Zipfel *et al.*, 2000; Mikouchi *et al.*, 2001; Wadhwa *et al.*, 2001). The groundmass of these olivine-bearing basaltic shergottites is mainly composed of two pyroxenes (pigeonite and augite) and plagioclase glass, and is similar to that of classic basaltic shergottites. Prior to the discovery of these African basaltic shergottites with megacrystic olivines, lithology A of EETA79001 was the only basaltic shergottite that contains olivine as a major constituent. In the case of EETA79001, several lines of petrological and chemical evidence point to a xenocrystic origin for the olivine megacrysts (McSween and Jarosewich, 1983; Steele and Smith, 1982; Mittlefehldt *et al.*, 1999). The presence of olivines in these shergottite meteorites is important because olivines in lherzolitic shergottites have similar chemical compositions in both major and minor elements to those in EETA79001 (*e.g.*, Harvey *et al.*, 1993; Ikeda, 1994; Treiman *et al.*, 1994; Mikouchi and Miyamoto, 2000) and thus, may suggest genetic relationships. The lherzolitic shergottites (Table 1) show a poikilitic texture composed of oikocrystic pyroxenes enclosing rounded to euhedral olivines. Interstitial olivines, pyroxenes, and plagioclase glass are also present between the poikilitic areas (*e.g.*, McSween, 1994). Since the three samples (ALH-77005, LEW88516, and Yamato-793605) of this shergottite group have nearly identical mineralogy, chemical compositions and ages (*e.g.*, Harvey *et al.*, 1993; Ikeda, 1994; Treiman *et al.*, 1994; Mikouchi and Miyamoto, 2000; Borg *et al.*, 2001a), they are believed to have come from the same igneous body.

Dhofar 019, a 1056 g single stone, is one of the newly discovered martian meteorites from Oman (Grossman, 2000; Taylor *et al.*, 2000). It is a basaltic shergottite mainly composed of pyroxene, plagioclase glass (“maskelynite”), and olivine (*e.g.*, Taylor *et al.*, 2000). Dhofar 019 is distinct from both classic basaltic shergottites and other African shergottites (Dar al Gani and Sayh al Uhaymir samples) in olivine and pyroxene mineralogy and may help clarify a petrogenetic relationship among these shergottites and the origins of olivine megacrysts. In this paper, we report a mineralogical study of Dhofar 019, paying special attention to chemical zoning of olivine and pyroxene and discussing the origin of olivine in this meteorite and relationship to other shergottites. In order to discuss the relationship to other basaltic shergottites, we selected Zagami, EETA 79001 (lithology A), and Dar al Gani 476, because these samples are distinct from each other in mineralogy and isotopic chemistry, and derive from different sources (*e.g.*, Mikouchi *et al.*, 1999, 2001; Borg *et al.*, 2001b). Also, to better understand the formation conditions of Dhofar 019, we used the Fe-Mg zoning profile of olivine grains to estimate a cooling rate for Dhofar 019.

2. Samples and analytical techniques

We prepared a thin section (*ca.* 4 × 4 mm) from a small rock chip of Dhofar 019 and analyzed it by the following methods. Backscattered electron (BSE) images were taken

with a JEOL JXA 840 and Hitachi S-4500 (field emission gun) scanning electron microscopes with energy dispersive spectrometers (EDS) (Dept. of Earth and Planet. Sci., University of Tokyo). Elemental distribution maps were acquired by a JEOL JXA 8900L electron microprobe (Dept. of Earth and Planet. Sci., University of Tokyo). Accelerating voltage was 15 kV, and the beam current was 80 nA. Modal abundances of minerals were calculated by combination of Si (pyroxenes and plagioclase), Mg (olivine and pyroxenes), Fe (olivine, pyroxenes and opaque phases), Ca (augite and Ca phosphates), Al (plagioclase), Ti (ilmenite), Na (plagioclase), and Cr (chromite) (X-ray maps of a 3×3 mm area). Quantitative wavelength dispersive analyses were performed on a JEOL Superprobe 733 electron microprobe (Ocean Research Institute, University of Tokyo) and a JEOL JCM 733 mk II (Dept. of Earth and Planet. Sci., University of Tokyo) microprobe by using natural and synthetic standards. Microprobe analyses of most phases were obtained at 15 kV accelerating voltage with a beam current of 12 nA. A defocused beam ($10 \mu\text{m}$ in diameter) and lower probe current (8 nA) were employed for the analysis of plagioclase glass to minimize volatile loss (*e.g.*, Mikouchi *et al.*, 1999). Dhofar 019 mineral compositions were compared with other shergottites using data from Mikouchi *et al.* (1999) (Zagami and EETA 79001), Mikouchi *et al.* (2001) (EETA 79001 and Dar al Gani 476), and Mikouchi and Miyamoto (2000) (ALH-77005, LEW 88516, and Yamato-793605).

3. Petrography

The thin section studied shows a pyroxene-dominant doleritic texture with evidence for strong shock metamorphism (*e.g.*, maskelynitization of plagioclase, micro-faults, undulatory and mosaic extinction of pyroxene and olivine, rare impact melt pockets) (Fig. 1a). As with other shergottites found in desert regions, the fractures in olivines are often filled with calcite formed by terrestrial weathering during residence in hot deserts (*e.g.*, Crozaz and Wadhwa, 2001). Although the section studied was fairly small, even within this restricted area, we observed slight textural variations. In one region, pyroxenes are more dominant relative to plagioclase glass than in the other part of the section. Clear differences in plagioclase composition are observed between the two areas (Fig. 2). The pyroxene-dominant area has more Na-rich plagioclase glass than the other area. Ca phosphate is also abundant in this area. However, the grain sizes are almost indistinguishable between the two areas. It is unclear whether both these lithologies are prevalent throughout Dhofar 019 or if the pyroxene-dominated area is present only in this section. Moreover, Taylor *et al.* (2000) reported a plagioclase-dominant area with finer-grained texture. Thus, Dhofar 019 may contain multiple lithologies like Zagami and EETA 79001 (McSween and Jarosewich, 1983; McCoy *et al.*, 1999).

The modal abundances of minerals in the entire section are 53.2% pigeonite, 11.4% augite, 19.5% plagioclase glass, 13.7% olivine, 1.0% Ca phosphates, 1.0% chromite, and 0.2% ilmenite (Fig. 2). Taylor *et al.* (2000) reported approximately similar modal abundances.

Olivine is present both as individual euhedral grains or as composite grains of ~ 0.5 mm in size. In our thin section, the largest grain is 1 mm long in maximum dimension. Olivine often shows brownish appearance along fractures, similar to olivines in lherzolitic shergottites (Ostertag, 1984; Treiman *et al.*, 1993). Magmatic inclusions ($\sim 100 \mu\text{m}$) are

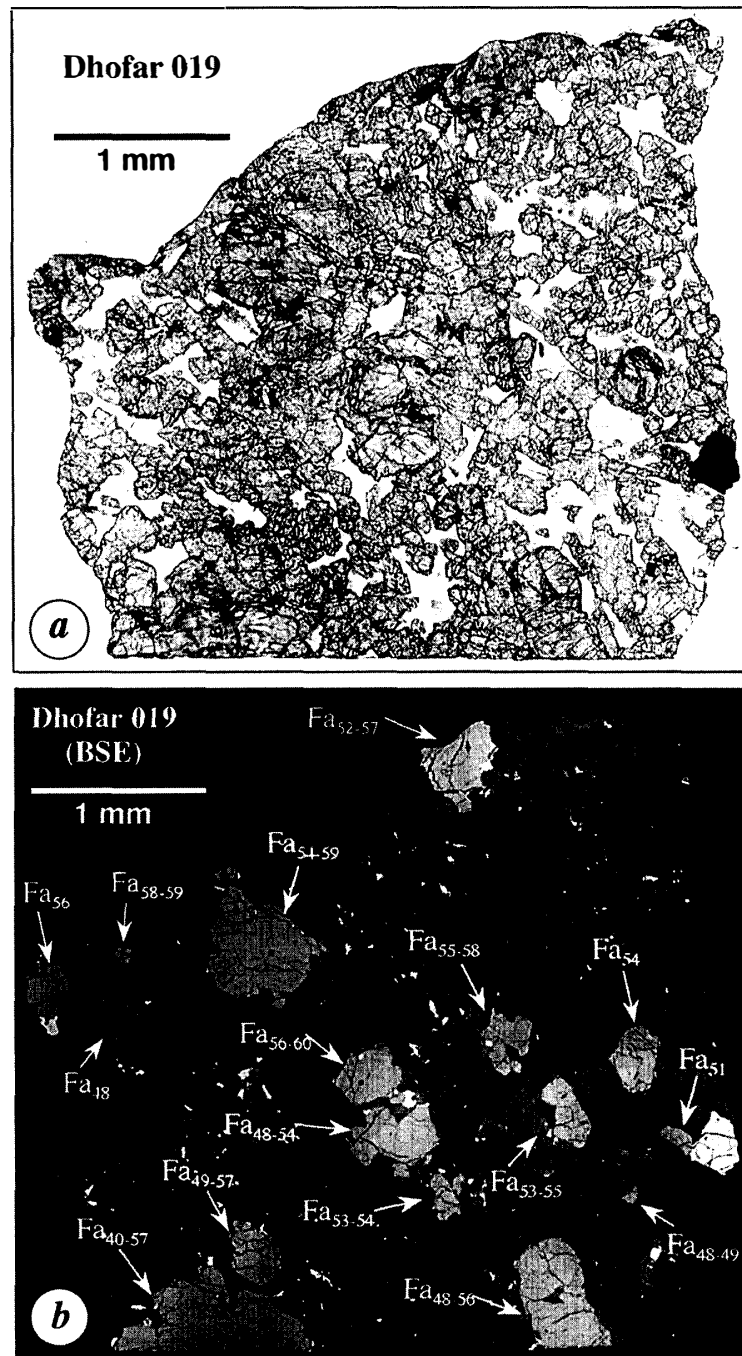


Fig. 1. (a) Optical photomicrograph (open nicol) of the Dhofar 019 thin section studied. The thin section shows a doleritic texture mainly composed of pyroxenes, plagioclase glass, and olivine. A large opaque phase ($\sim 200 \mu\text{m}$) at the right edge of the section is chromite with a zoned Fe, Ti-rich rim. (b) Backscattered electron image of the Dhofar 019 thin section studied. Bright phases with variable contrasts are olivines. Their compositions are indicated in the image.

common in olivines. Pyroxenes are euhedral to subhedral, usually 0.2–0.5 mm long, and show polysynthetic twinning. An additional population of smaller pyroxene grains ($\sim 100 \mu\text{m}$) appears abundant. Lentz *et al.* (2001) reported a remarkable similarity in crystal

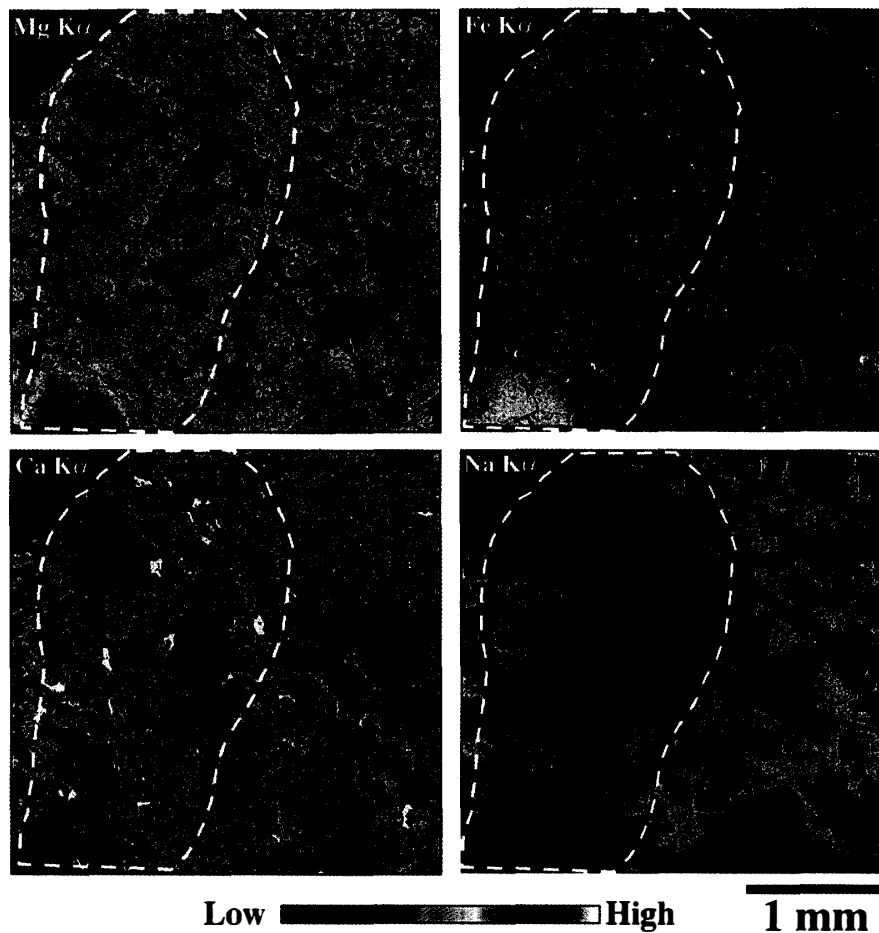


Fig. 2. Mg, Fe, Ca, and Na X-ray maps of the Dhofar 019. Orange-yellow phases in the Fe image are olivines. The area surrounded by dashed lines is pyroxene dominated and has plagioclase that is more Na-rich. This area is also abundant in Ca phosphates (small white phases in Ca K α image). The Na map shows irregular zoning patterns of plagioclase glass.

size distributions (CSD) of pyroxenes between Dhofar 019 and Zagami. Plagioclase is subhedral to anhedral, typically up to 0.5 mm long, and is optically isotropic. It does not show any evident fractures like the “maskelynite” in other shergottites. Minor phases are Ca phosphates, chromite, ulvöspinel, ilmenite, and pyrrhotite. We observed one euhedral chromite grain (200 μm across) with a zoned Fe, Ti-rich rim.

4. Mineral chemistry

Representative mineral compositions are given in Table 2.

4.1. Olivine

The largest olivine grain we observed has a Fa₄₀ core composition and is zoned towards a Fa₅₇ rim. This is the most magnesian olivine in the thin section and its core composition is identical to the most magnesian olivine reported by Taylor *et al.* (2000). Although they reported more ferroan olivines (\sim Fa₇₅), we did not find olivines more

Table 2. Representative mineral compositions of major phases in Dhofar 019 shergottite.

	Olivine (Mg-rich)	Olivine (Mg-poor)	Pigeonite (Mg-rich)	Pigeonite (Mg-poor)	Augite (Mg-rich)	Augite (Mg-poor)	Plagioclase (An-rich)	Plagioclase (An-poor)	Merrillite	Chromite	Ulvospinel	Ilmenite
SiO ₂	36.41	34.34	54.01	50.66	53.42	51.04	52.41	57.84	0.19	0.13	0.04	0.04
Al ₂ O ₃	0.00	0.01	1.13	0.50	1.24	0.84	29.38	25.57	0.04	7.76	2.53	0.01
TiO ₂	0.03	0.07	0.06	1.12	0.22	0.98	0.02	0.10	0.22	0.59	30.91	53.64
FeO	34.03	46.58	15.48	25.89	11.44	20.00	0.49	0.41	2.65	26.57	59.84	41.30
MnO	0.68	0.87	0.54	0.78	0.38	0.73	0.06	0.00	0.15	0.59	0.63	0.75
MgO	28.12	17.88	25.09	15.69	18.33	11.84	0.18	0.07	3.05	5.27	1.32	2.39
CaO	0.22	0.32	3.26	5.22	14.38	13.95	14.11	9.26	44.17	0.03	0.05	0.19
Na ₂ O	0.01	0.00	0.07	0.05	0.10	0.19	3.75	6.17	0.74	0.00	0.00	0.00
K ₂ O	0.02	0.02	0.00	0.01	0.00	0.00	0.06	0.36	0.00	0.00	0.02	0.02
Cr ₂ O ₃	0.00	0.12	0.49	0.19	0.69	0.27	0.00	0.03	0.05	58.14	3.85	0.57
V ₂ O ₃	0.02	0.00	0.01	0.11	0.03	0.11	0.00	0.00	0.00	0.39	0.26	0.27
NiO	0.00	0.00	0.02	0.01	0.00	0.01	0.01	0.11	0.00	0.00	0.00	0.00
P ₂ O ₅	0.00	0.07	0.02	0.02	0.13	0.00	0.00	0.00	46.75	0.00	0.00	0.00
Total	99.54	100.29	100.16	100.25	100.35	99.95	100.48	99.91	98.01	99.47	99.43	99.18
<i>Fs</i>			24.0	42.8	18.3	33.9						
<i>En</i>			69.5	46.2	52.2	35.8						
<i>Wo</i>			6.5	11.0	29.5	30.3						
<i>fe#*</i>	0.404	0.594	0.257	0.481	0.259	0.487						
<i>An</i>							67.3	44.4				
<i>Ab</i>							32.3	53.5				
<i>Or</i>							0.4	2.1				

**fe#* = Atomic Fe/(Fe+Mg)

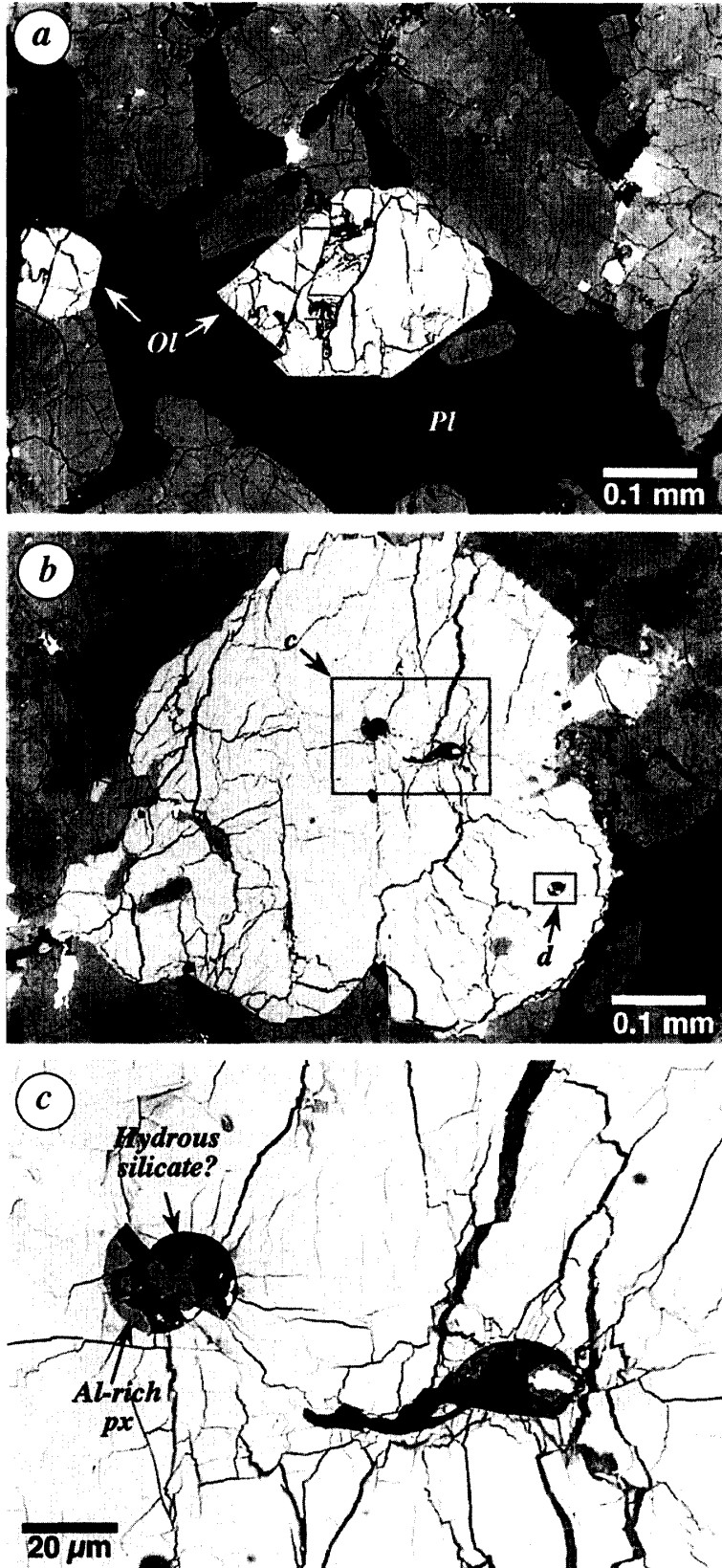


Fig. 3.

- (a) Backscattered electron image of the small euhedral olivine grains (Ol) in Dhofar 019. The olivine grain at the center of the image is faulted possibly due to shock. Px: pyroxene. Pl: plagioclase glass.
- (b) Backscattered electron image of one of the large non-euhedral olivine grains in Dhofar 019. This grain contains several types of magmatic inclusions both at the center and the rim of the host olivine grain.
- (c) Two magmatic inclusions near the center of the host olivine. Both inclusions contain a hydrous silicate? (dark areas) and Al-rich pyroxenes. Fractures in olivine are filled with calcite.

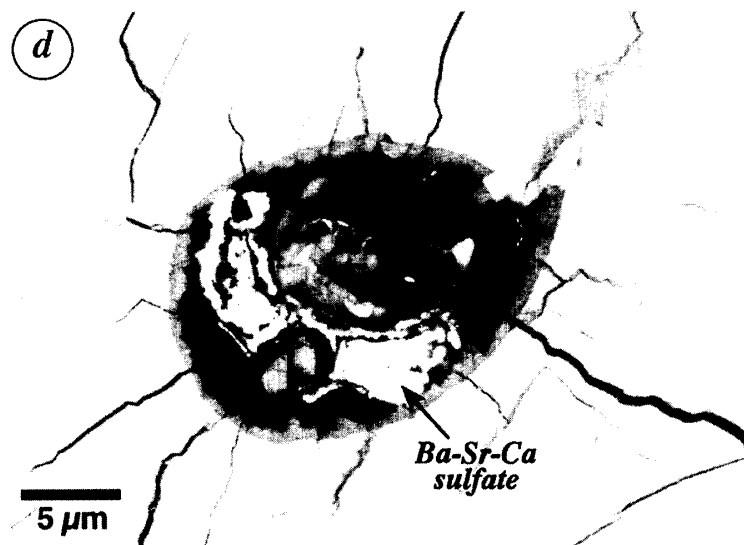


Fig. 3. Continued.

(d) One of the unique magmatic inclusions contains (Ba, Sr, Ca) sulfate, probably of terrestrial origin.

ferroan than Fa_{59} . Some small olivine grains show euhedral shapes (Fig. 3a) and are rather homogeneous within each grain, but compositional variation is observed from one grain to another (Fa_{48-58}). Figure 1b shows the variation of olivine compositions in the section studied. The CaO content is 0.3–0.4 wt%. Al_2O_3 is generally less than 0.05 wt%, but some analyses (especially in the brownish regions) give ~0.8 wt% Al_2O_3 . Magmatic inclusions (~100 μm) are often observed in large olivine grains. These are usually near the centers of the host olivine grains, but some inclusions are located near the rims (Fig. 3b). The most common inclusions are composed of pyroxenes and feldspathic glass. Pyroxenes are pigeonite ($\text{En}_{68}\text{Fs}_{27}\text{Wo}_5$ – $\text{En}_{52}\text{Fs}_{37}\text{Wo}_{11}$) and augite (~ $\text{En}_{40}\text{Fs}_{27}\text{Wo}_{33}$). Their compositions roughly overlap phenocrystic pyroxenes. Al-rich pyroxenes are also observed (~5 wt% Al_2O_3), sometimes rimming the walls of the inclusions. A few inclusions contain a magnesian silicate phase (41–43 wt% SiO_2 , 8–9 wt% Al_2O_3 , 1 wt% TiO_2 , 1.5–2.0 wt% FeO, 26–28 wt% MgO, 2–4 wt% CaO, 0.1–0.2 wt% Na_2O , 0.2–0.3 wt% K_2O) with analytical totals of only 83–88 wt% (Fig. 3c). It is likely that this is a hydrous phase, and its cation ratio is roughly similar to that of vermiculite. However, other analytical techniques (*e.g.*, micro-areas infrared spectroscopy) are required to confirm the hydrous nature. Another unusual phase noted is a (Ba, Sr, Ca)-sulfate (Fig. 3d). Gypsum is found in some types of martian meteorites and is possibly of martian origin (*e.g.*, Gooding *et al.*, 1988). It is not certain whether these unique phases in Dhofar 019 are of martian origin or not, but the long terrestrial age of this meteorite (0.34 ± 0.04 Ma) suggests origin by terrestrial weathering during long residence in the hot desert (Nishiizumi *et al.*, 2002). Calcite is commonly present along fractures, strongly suggesting that water has percolated throughout this rock.

4.2. Pyroxenes

Both pigeonite and augite are present, and both are extensively zoned from magnesian cores to ferroan rims. Spatial distributions of pigeonite and augite are complex due to their complicated zoning patterns. It appears that pigeonite and augite are sometimes present as separate grains. However, some augite is present partially

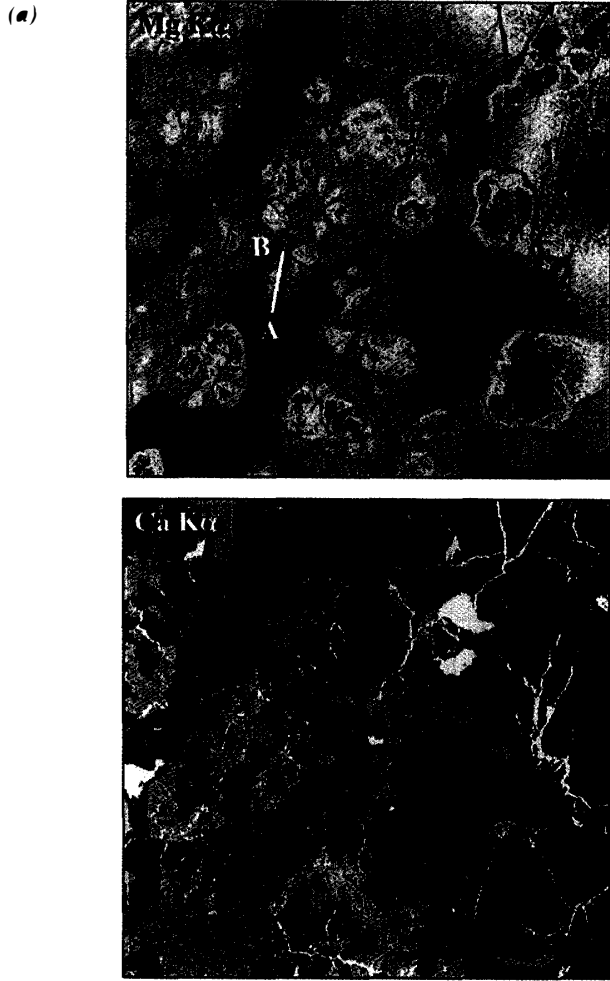
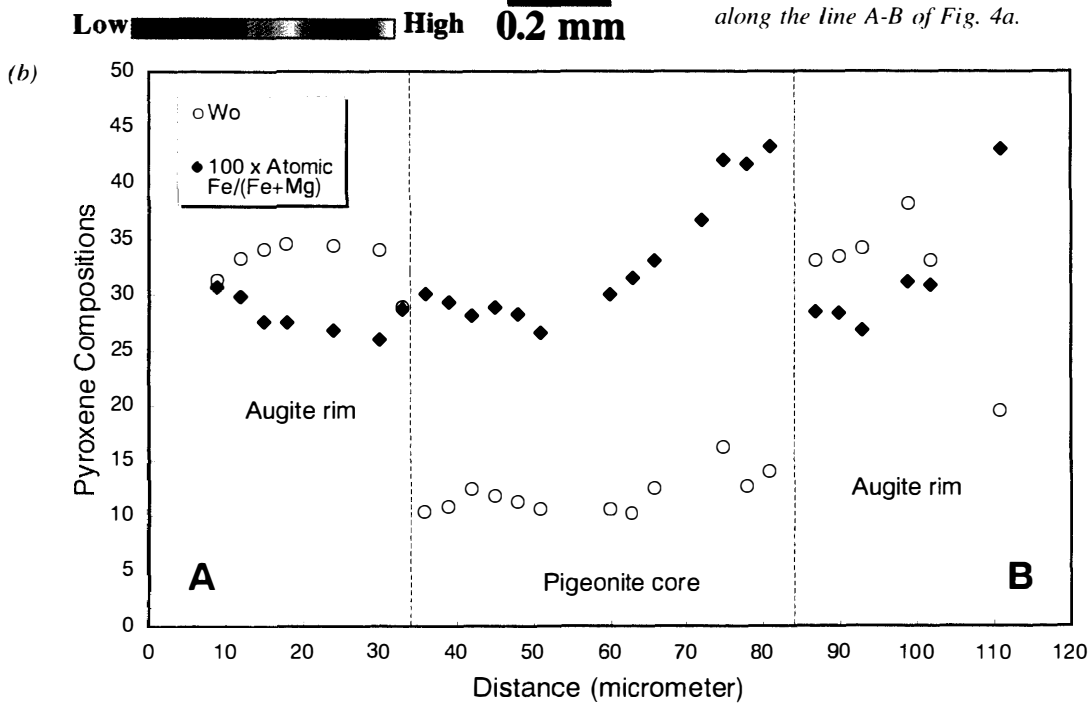


Fig. 4.
 (a) Mg and Ca X-ray maps of the Dhofar 019, showing complex pyroxene zoning features. The line A-B in the Fig. 4a indicates a small pyroxene grain that shows obvious rimming of augite surrounding pigeonite core.
 (b) The zoning profiles for $fe\#$ and the Wo content of the pyroxene along the line A-B of Fig. 4a.



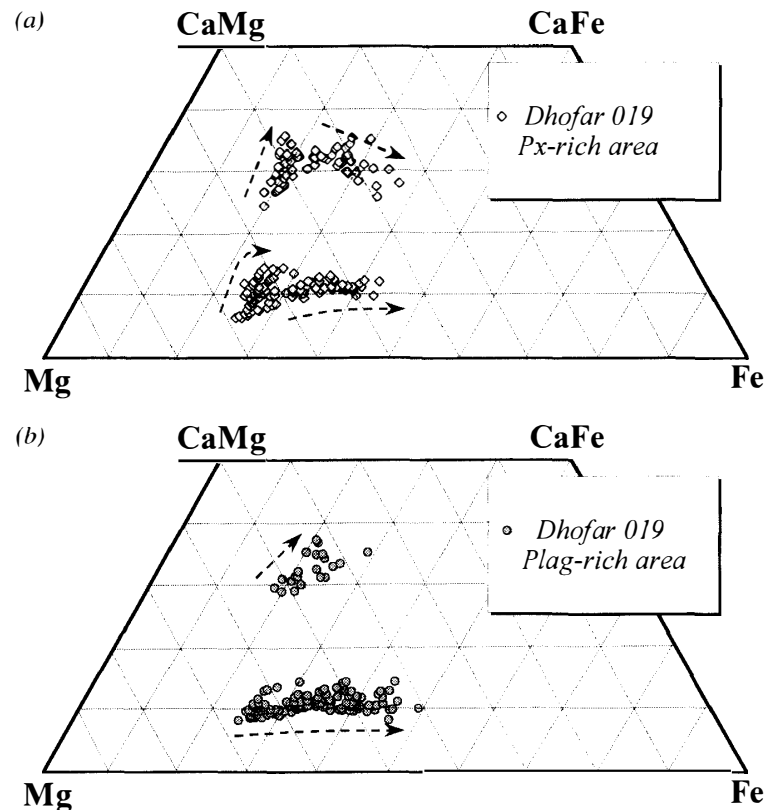


Fig. 5. Pyroxene quadrilaterals from two different areas of Dhofar 019. (a) Plots from the pyroxene-dominated area. (b) Plots from the plagioclase-dominated area. No significant differences in pyroxene compositions are observed among them except for the presence of ferroan augites in the pyroxene-dominated area.

rimming the magnesian pigeonite cores (Fig. 4). Figure 5 shows pyroxene compositions from the two areas in Dhofar 019. For pigeonite, we do not see a large difference between two areas, but augite in the pyroxene-dominant area extends to more Fe-rich compositions than that of the plagioclase-dominant area (Fig. 5). Moreover, augite is less abundant in the plagioclase-dominant area. Furthermore, two compositional trends are observed for both pigeonite and augite from the pyroxene-dominant area. Pigeonites range from $\text{En}_{69}\text{Fs}_{25}\text{Wo}_6$ to $\text{En}_{60}\text{Fs}_{25}\text{Wo}_{15}$ and from $\text{En}_{58}\text{Fs}_{31}\text{Wo}_{11}$ to $\text{En}_{45}\text{Fs}_{42}\text{Wo}_{13}$ (Fig. 5). Augites range from $\text{En}_{53}\text{Fs}_{20}\text{Wo}_{27}$ to $\text{En}_{48}\text{Fs}_{17}\text{Wo}_{35}$ and from $\text{En}_{45}\text{Fs}_{22}\text{Wo}_{33}$ to $\text{En}_{37}\text{Fs}_{32}\text{Wo}_{31}$ (Fig. 5). Pyroxenes in the plagioclase-dominant area overlap these compositions. Al and Ti in pyroxenes also show two trends. Al_2O_3 in pigeonites first increases from 0.6 wt% ($fe\#=0.27$) to 1.2 wt% ($fe\#=0.3$), and then decreases from 1.2 wt% ($fe\#=0.33$) to 0.6 wt% ($fe\#=0.5$) (Fig. 6a). Al_2O_3 in augites shows an increase from 1.2 wt% ($fe\#=0.26$) to 2.0 wt% ($fe\#=0.3$), and then a decrease from 1.8 wt% ($fe\#=0.32$) to 1.0 wt% ($fe\#=0.5$) (Fig. 6b). TiO_2 is nearly homogeneous in magnesian pyroxenes (pigeonite: 0.1 wt%, augite: 0.2 wt%), but ferroan pyroxenes show Ti increase with increasing $fe\#$ (pigeonite: 0.2–0.7 wt%, augite: 0.3–1.0 wt%) (Fig. 6). The onset of the Ti increase occurs at around $fe\#=0.33$, nearly coincident with the maximum Al content. The subsequent drop of Al probably corresponds with the onset of plagioclase crystallization as is seen in other

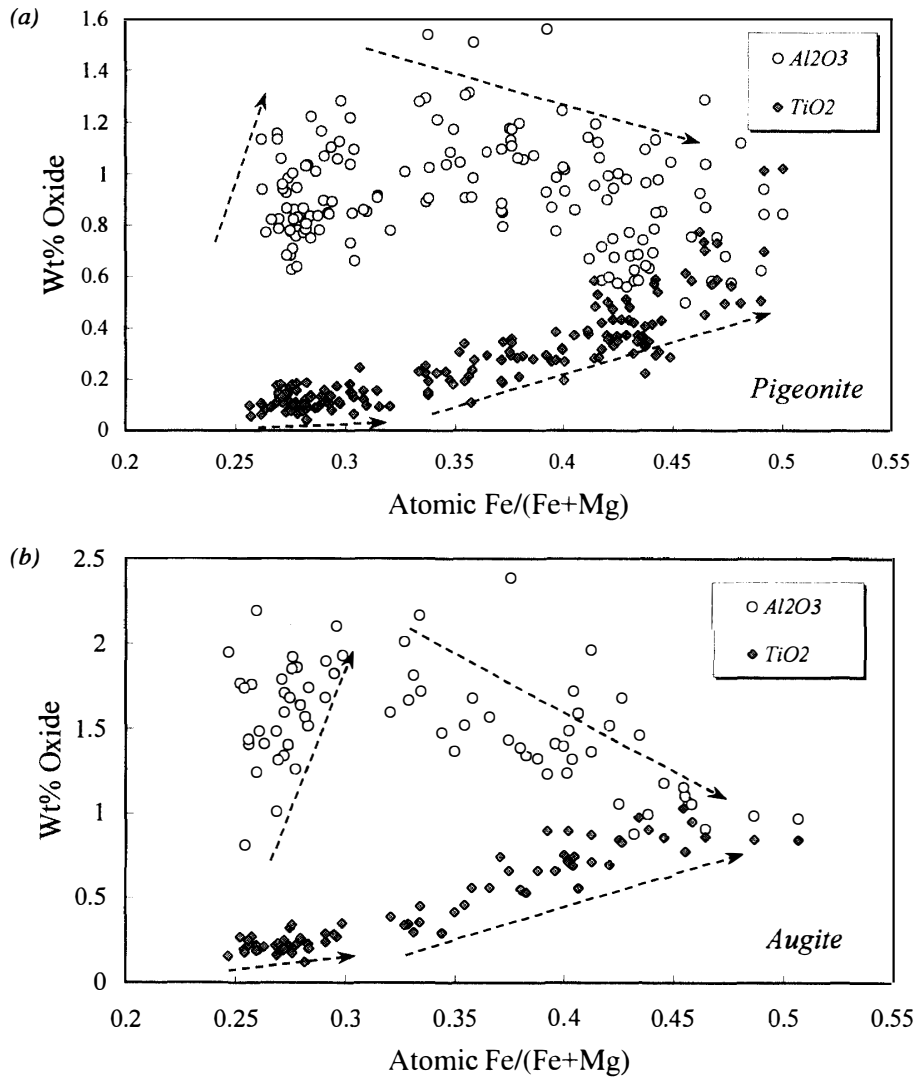


Fig. 6. (a) Al and Ti variations of pigeonites in Dhofar 019. A compositional kink is observed at around $fe\# = 0.30-0.33$ both for Al and Ti. (b) Al and Ti variations of augites in Dhofar 019. A compositional kink is also observed at around $fe\# = 0.30-0.32$.

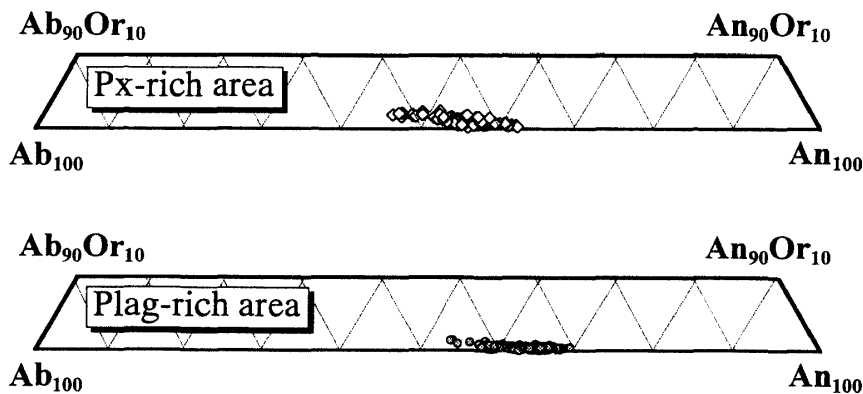


Fig. 7. Plagioclase quadrilaterals from two different areas of Dhofar 019. Plagioclase glass in the pyroxene-dominated area is clearly more Ab-rich than that in the plagioclase-dominated area.

shergottite pyroxenes (*e.g.*, Mikouchi *et al.*, 1999). Alternatively, it may mark the incorporation of xenocrysts or another magma.

4.3. Plagioclase

There is a clear difference in plagioclase composition between two areas as stated above. The pyroxene-dominant area has more Na-rich compositions ($An_{61}Ab_{38.5}Or_{0.5}$ to $An_{44}Ab_{54}Or_2$) than the plagioclase-dominant area ($An_{68}Ab_{31.5}Or_{0.5}$ to $An_{52}Ab_{46.5}Or_{1.5}$) (Fig. 7). However, there is no clear difference in FeO content of plagioclase (0.2–0.7 wt%). Plagioclase zoning patterns are irregular due to their subhedral to anhedral grain shapes (Fig. 2). Many plagioclase grains do not display complete concentric compositional zones. Instead, the most calcic part is usually near grain boundaries to pyroxene and olivine, suggesting that plagioclase may have nucleated on other minerals and grown outward into the melt.

4.4. Minor Phases

One large chromite grain has a homogeneous composition (58 wt% Cr_2O_3 , 27 wt% FeO, 8 wt% Al_2O_3 , 5 wt% MgO) except for a thin zoned Fe, Ti-rich rim (20 wt% TiO_2 , 21 wt% Cr_2O_3 , 50 wt% FeO, 4 wt% Al_2O_3 , 2 wt% MgO) (Fig. 8). Small grains (~100 μm) of ulvöspinel (30 wt% TiO_2 , 4 wt% Cr_2O_3 , 60 wt% FeO, 3 wt% Al_2O_3 , 1 wt% MgO) and zoned Fe, Ti-rich spinel (22–24 wt% TiO_2 , 16–20 wt% Cr_2O_3 , 48–52 wt% FeO, 4 wt% Al_2O_3 , 2 wt% MgO) are scattered in the thin section (Fig. 8). Ilmenite (~100 μm) contains ~2.5 wt% MgO. Merrillite is typically homogeneous and gives the composition of $Ca_{8.9}(Mg,Fe)_{1.1}Na_{0.3}(PO_4)_7$.

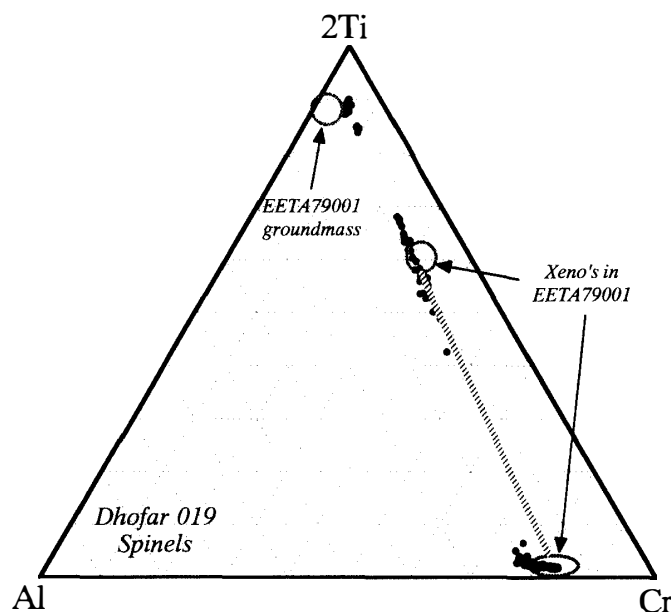


Fig. 8. Spinel compositions from Dhofar 019. The dashed areas are from spinels in lithology A of EETA 79001. Note that a chromite xenocryst with Ti-rich rim in EETA79001 is nearly identical to the large chromite grain observed in Dhofar 019. The groundmass ulvöspinel is also similar in composition.

5. Comparison with other shergottites

Dhofar 019 shows several mineralogical similarities to the previously known basaltic shergottites. However, clear differences are observed. In this chapter, we compare mineralogy of Dhofar 019 with other basaltic shergottites as well as lherzolitic shergottites.

One of the most remarkable mineralogical characteristics of Dhofar 019 is the presence of abundant olivine grains with variable sizes and compositions (Fig. 1b). Generally, the larger grains show chemical zoning from magnesian cores to ferroan rims, and the smaller grains are homogeneous with ferroan compositions. This is probably due to the effect of off-center cuts of large grains. However, we note that the homogeneous compositions of small olivine grains are different from one grain to another, covering the range Fa_{48-59} . Compositionally, Dhofar 019 olivines are too Fe-rich to be in equilibrium with the pyroxene cores. Dhofar 019 pyroxene cores have $fe\# = 0.27$. If we use the $Kd^{Atomic (Fe/Mg)}_{\text{olivine/pigeonite}}$ of 1.24 obtained from crystallization experiments on synthetic QUE 94201 (Koizumi *et al.*, unpublished data), olivine of Fa_{55} would be in equilibrium with pigeonite of $fe\# = 0.5$. The most magnesian olivine core (Fa_{40}) would be in equilibrium with pigeonite of $fe\# = 0.35$, significantly more Fe-rich than the Dhofar pyroxene cores ($fe\# = 0.27$). It is also puzzling that olivines show variable grain shapes from nearly euhedral grains (Fig. 3a) to rather anhedral grains (Fig. 3b). Well-defined euhedral shapes are found only in small grains (Fig. 1b). Taylor *et al.* (2000) suggested that Dhofar 019 olivines could be xenocrysts trapped by a parent melt. Because of their disequilibrium compositions, variable sizes, and unusual compositional populations, we also suggest that some olivines are xenocrysts. Based on crystal size distributions, Lentz *et al.* (2001) pointed out that olivines have two distinct populations with different origins. However, the section studied here is small, and further systematic study of larger thin sections is required to explore the origin of olivines.

Except for EETA79001, olivine has been a rare component in basaltic shergottites until the recent discoveries of Dar al Gani and Sayh al Uhaymir shergottites (Table 1). In EETA79001, olivine is magnesian (Fa_{19-45}) and is interpreted to be a xenocryst (*e.g.*, Steele and Smith, 1982; McSween and Jarosewich, 1983). In Dar al Gani and Sayh al Uhaymir picritic shergottites, olivines also occur as large grains reaching several millimeters long, and their compositions are Fa_{24-42} (*e.g.*, Folco *et al.*, 2000; Zipfel *et al.*, 2000; Mikouchi *et al.*, 2001; Wadhwa *et al.*, 2001). In contrast to the case of EETA 79001, the origins of olivine megacrysts in these desert shergottites have been under dispute (*e.g.*, Folco *et al.*, 2000; Zipfel *et al.*, 2000; Mikouchi *et al.*, 2001; Wadhwa *et al.*, 2001). Lherzolitic shergottites contain olivines (~1 mm) compositionally similar (Fa_{26-35}) to those in EETA 79001 and Dar al Gani/Sayh al Uhaymir shergottites (*e.g.*, Harvey *et al.*, 1993; Ikeda, 1994; Treiman *et al.*, 1994; Mikouchi and Miyamoto, 2000). In lherzolitic shergottites, rounded to euhedral olivine grains are enclosed in large oikocrystic pyroxenes and these olivines are fairly homogeneous. The crystallization of olivine started prior to that of pyroxene, and olivines were trapped within pyroxenes, forming a poikilitic texture. Although it is not obvious whether olivines in lherzolitic shergottites are related to those in EETA 79001 and Dar al Gani/Sayh al Uhaymir, they

have in common that their olivines contain magmatic inclusions composed of Al-rich pyroxenes and feldspathic glasses. It is interesting that Dhofar 019 olivines also contain magmatic inclusions composed of Al-rich pyroxenes and feldspathic glass. However, in comparison with olivines in EETA79001, Dar al Gani/Sayh al Uhaymir, and Iherzolitic shergottites, Dhofar 019 olivines are much more ferroan and clearly distinct. The CaO content (0.3–0.4 wt%) of the Dhofar 019 olivines is slightly higher than those of EETA 79001, Dar al Gani/Sayh al Uhaymir, and Iherzolitic shergottites are (*e.g.*, Mikouchi and Miyamoto, 2000; Mikouchi *et al.*, 2001). In Dar al Gani 476, small olivines have the same ferroan composition, whereas in Dhofar 019 small olivines vary in composition from grain to grain (Zipfel *et al.*, 2000). Thus, Dhofar 019 olivines are different from Dar al Gani 476 olivines.

In contrast with olivines, pyroxenes in Dhofar 019 show several similarities to other basaltic shergottites. The pyroxene compositions of Dhofar 019 overlap those of Dar al Gani 476 in the magnesian regions and Zagami in the ferroan regions (Fig. 9). They are also similar to lithology A of EETA79001 in the magnesian regions (Fig. 9). However, minor element contents (Al and Ti) are different from both Dar al Gani 476 and Zagami (Fig. 10). They are rather closer to pyroxenes in lithology A of EETA 79001 (Fig. 10). We note that the compositional kinks of Al and Ti are nearly identical between Dhofar 019 and lithology A of EETA79001 (Fig. 10). The presence of augite rimming the pigeonite cores, though it is not always clear in Dhofar 019, is known in other basaltic shergottites. It is most distinct in the QUE94201 shergottite and is interpreted to be a product of metastable crystallization from the undercooled magmas (*e.g.*, Mikouchi *et al.*, 1998, 1999). Some pyroxenes in lithology A of EETA79001 also display similar zoning patterns, and in this respect, they have a common characteristic with Dhofar 019. In contrast, pigeonite and augite are present as separate grains in Shergotty and Zagami, suggestive of crystallization nearer in equilibrium (*e.g.*, Mikouchi *et al.*, 1999). However, McCoy *et al.* (1999) reported a much wider range of pyroxene compositions and McCoy *et al.* (1992) documented augite rimming Mg-rich Zagami pigeonite cores in many cases. The presence of several different lithologies in Zagami (McCoy *et al.*, 1992, 1999) may have brought about these differences. Therefore, we consider that Dhofar 019 crystallized from a slightly undercooled magma, as did lithology A of EETA79001 and Zagami. In fact, Lentz and McSween (2001) pointed out that Dhofar 019 is similar to Zagami and distinct from lithology A of EETA79001 and Dar al Gani 476 according to their crystal size distribution analysis for pyroxenes. Pyroxenes in Dhofar 019 extend to more ferroan compositions than lithology A of EETA79001 and show similar pyroxene zoning trends to Zagami in the late stages of crystallization (Fig. 9). Plagioclase zoning patterns in Dhofar 019 are closer to Zagami than EETA79001 because of their similarity in irregular, non-concentric zoning in subhedral to anhedral grains. Thus, pyroxenes and plagioclase in Dhofar 019 are similar to both lithology A of EETA79001 and Zagami, but differ in detail. In order to further discuss this topic, more detailed analysis (*e.g.*, trace element chemistry, isotopic compositions) will be required.

Spinel compositions in Dhofar 019 are comparable to those of lithology A of EETA 79001 and Iherzolitic shergottites (*e.g.*, McSween and Jarosewich, 1983; Zipfel *et al.*, 2000; Mikouchi and Miyamoto, 2000) (Fig. 8). Especially, the large chromite grain in Dhofar 019 shows a similar zoning trend to that in lithology A of EETA79001. Spinel

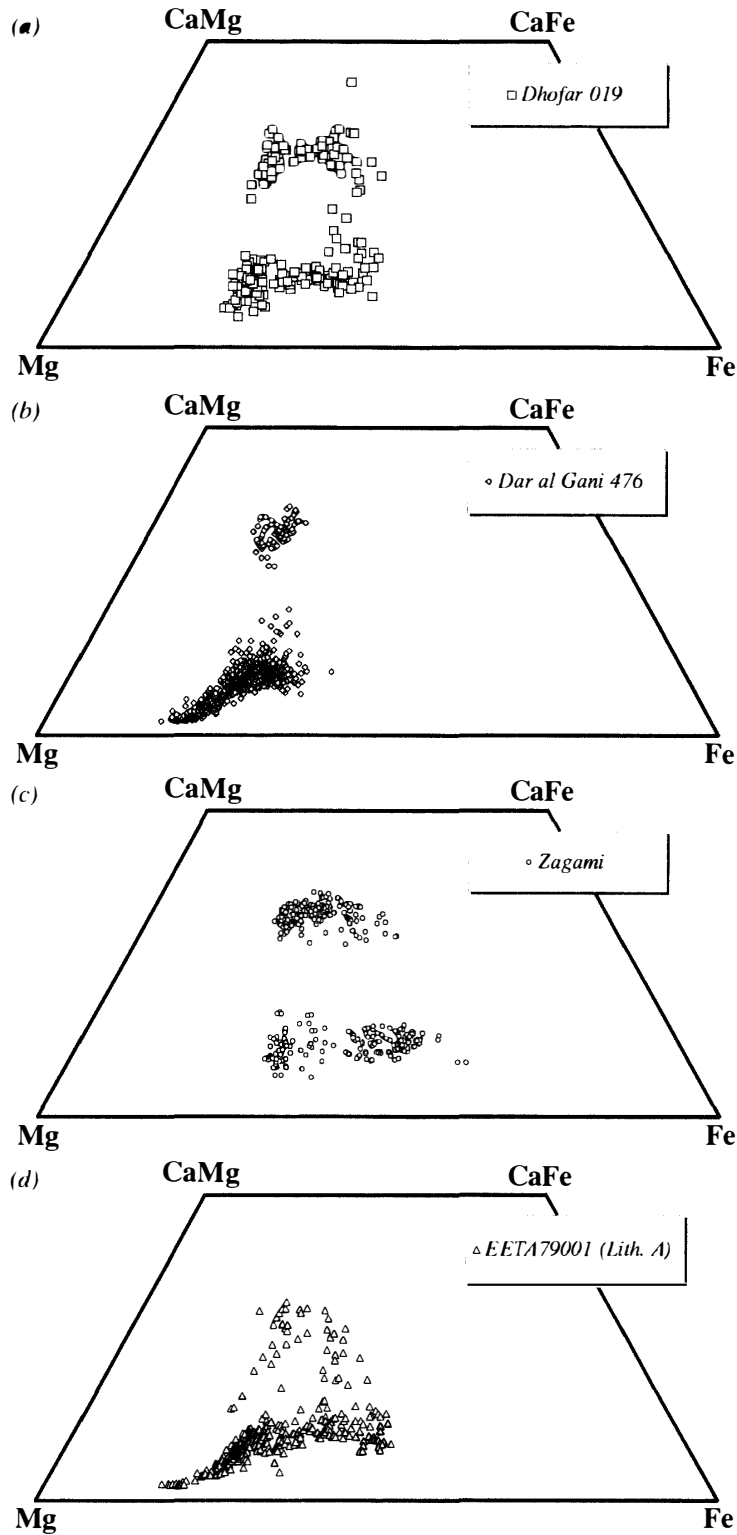


Fig. 9. Pyroxene quadrilaterals for (a) Dhofar 019, (b) Dar al Gani 476, (c) Zagami, and (d) EETA79001 (lithology A). Note that the pyroxene compositions of Dhofar 019 overlap those of Dar al Gani 476 and EETA79001 shergottites in the magnesian regions and Zagami in ferroan regions. The pyroxenes of lherzolitic shergottites are also overlapped in the magnesian regions, although they are not plotted.

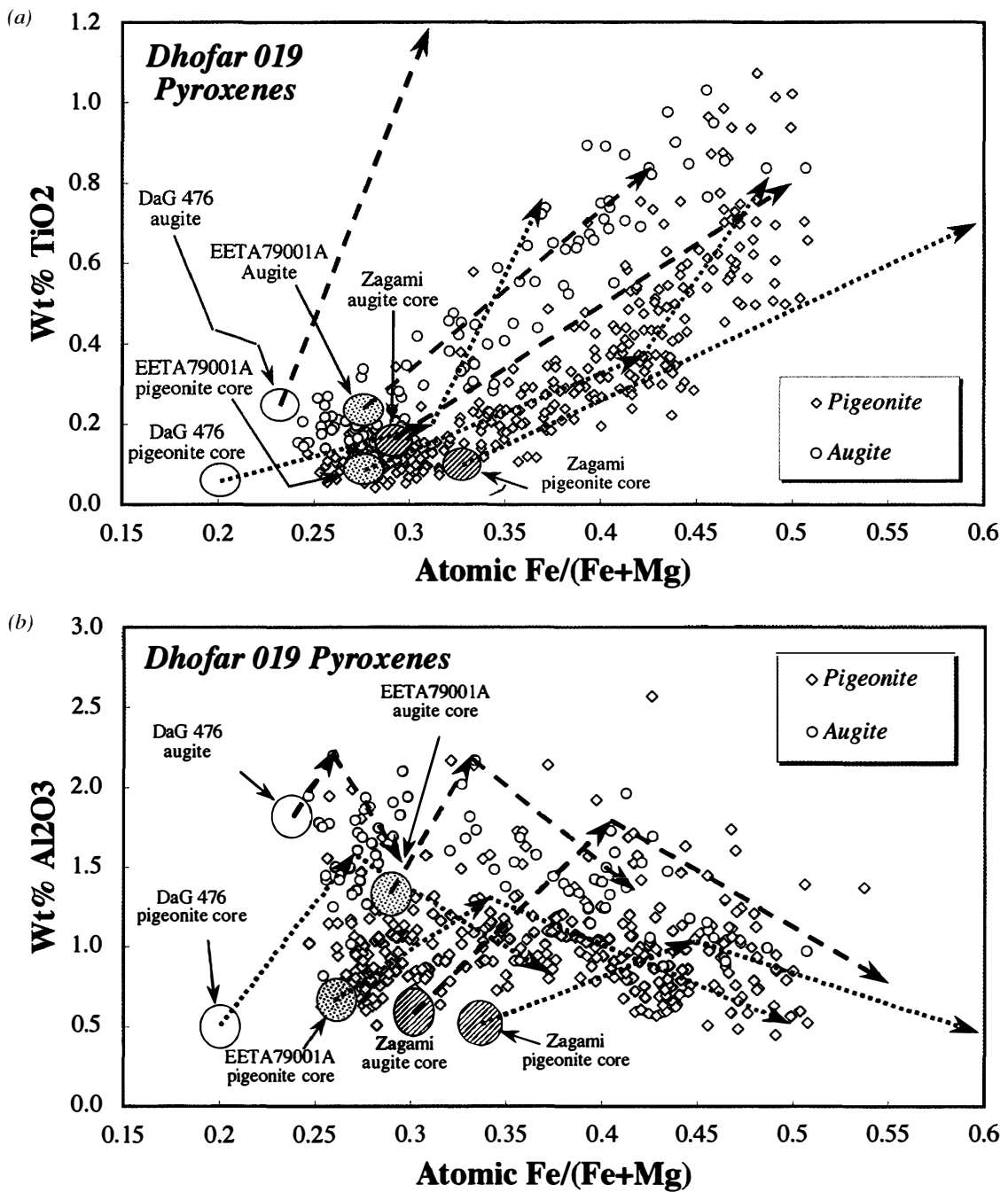


Fig. 10. (a) Ti variations of pigeonite and augite in Dhofar 019. (b) Al variations of pigeonite and augite in Dhofar 019. Note that EETA79001 (lithology A) shows nearly identical zoning trends and compositions to Dhofar 019. EETA79001A: lithology A of EETA79001. DaG 476: Dar al Gani 476.

in Dar al Gani and Sayh al Uhaymir shergottites also have generally similar compositions. Because chromite in lithology A of EETA79001 is interpreted to be xenocryst (*e.g.*, McSween and Jarosewich, 1983), chromites in Dhofar 019 may be also xenocrysts and may share the same origin.

The origin of homogeneous ferroan olivines with variable compositions is unclear. These olivines may be phenocrysts and may have crystallized with ferroan pyroxenes and plagioclase in the groundmass. If this is the case, their compositions may preserve the equilibrium compositions with the magma at different steps in the late-crystallization stages. Alternatively, they may be xenocrysts, and rapid cooling of the groundmass prevented them from being equilibrated. The presence of ferroan pyroxenes in Dhofar 019 might be explained by incorporation of ferroan magma with ferroan olivine xenocrysts into magnesian magma with magnesian olivine and pyroxenes at some time during its early crystallization stages. The adding of ferroan components might cause crystallization of ferroan pyroxenes. Nevertheless, it is impossible to conclude which model is correct only from this study.

6. Olivine cooling calculation

As chemical zoning is present in some large olivine grains and homogeneous olivines show different compositions from each other, Dhofar 019 appears to have experienced a rapid cooling history. We computed the Fe-Mg zoning profiles of olivine at various cooling rates (from 1200°C to 700°C) and compared the resultant profiles with that of the largest (most magnesian) olivine grain in Dhofar 019. We assumed that the olivine was initially homogeneous (about Fa_{25-30}) and the observed profile was achieved during crystallization of the groundmass due to interaction between olivine and the groundmass melt. We consider that the olivine is a xenocryst, and the obtained cooling rate would correspond to the cooling rate of the groundmass crystallization.

Although several data have been reported for Mg-Fe diffusion rate in olivine (*e.g.*, Buening and Buseck, 1973; Misener, 1974; Chakraborty, 1997), we used that of Misener (1974). This is because our diffusion experiment (Miyamoto and Mikouchi, 1998) gives the best fit between observed diffusion profiles and those using the diffusion rate from Misener (1974). The recently measured rate by Chakraborty (1997) is intermediate between the rate by Buening and Buseck (1973) and that by Misener (1974), but it is closer to Misener (1974) if we take the oxygen fugacity (fO_2) dependence into consideration (Miyamoto and Mikouchi, 2001). We revised the equation of Misener (1974) to include the effects of fO_2 and Fe/Mg ratios of olivine upon the diffusion rates (Miyamoto and Mikouchi, 1998). In this calculation, we employed fO_2 of one log unit above the iron wüstite buffer (IW+1). Although we terminated calculations when temperature reached 700°C, there is no significant difference in the result even if olivine cooled well below 700°C. This is because atomic diffusion slows dramatically at such low temperatures, so that profile modification is mostly achieved at high temperatures (>1100°C). We began our calculation at 1200°C. If olivine in Dhofar 019 actually cooled from an even higher temperature, as might be expected from the magnesian pyroxene compositions, then olivine would have experienced even faster cooling rates than the result obtained for the 1200–700°C temperature range.

The computed profiles suggest that cooling rates of 0.05–0.1°C/hour give the best fit to the observed zoning profile of the Dhofar 019 olivine. The cooling rate of 0.05–0.1°C/hour from 1200 to 700°C corresponds to the burial depth of ~5 m from the surface if we assumed that it was covered with rock-like materials (McKay *et al.*, 1998). If it was

covered with regolith-like materials, burial depths are much shallower due to lower thermal diffusivity (McKay *et al.*, 1998). Lentz and McSween (2001) also estimated a fast cooling rate (5–15 days of cooling) of the Dhofar 019 olivine by estimating a time necessary to homogenize olivines in Fe/Mg.

Because the original profile of the analyzed olivine is unknown (we assumed that it was homogeneous) and the olivine composition could be altered in magma prior to the crystallization of the groundmass, the obtained cooling rate could bear large uncertainties. However, the cooling rate calculations are not highly sensitive to the assumed original zoning profiles (either homogeneous or zoned); the obtained cooling rates usually agree within in an order of magnitude. Therefore, we believe that the obtained cooling rate in this study gives meaningful cooling rate information.

A shallow geological setting of the Dhofar 019 magma implies that it crystallized in a lava flow. EETA79001 and Dar al Gani 476 have generally similar cooling rates (0.4–0.5°C/hour) to that of Dhofar 019 (Mikouchi *et al.*, 2001). The source of heat that generated the magma is not clear. Impact melting can explain such a shallow setting for the magma as Mittlefehldt *et al.* (1999) proposed for lithology A of EETA79001. Impact melting and subsequent rapid cooling could explain the presence of homogeneous olivines with variable compositions. However, endogenous melting is also possible as Mars is a large, geologically active planet laden with lava flows. Therefore, it may be possible that mixing of magnesian magma (with magnesian olivines and pyroxenes) and ferroan magma (with ferroan olivines) produced Dhofar 019.

7. Conclusions

Thus, Dhofar 019 shows similarities to both lithology A of EETA79001 (*e.g.*, pyroxene compositions, spinel compositions, cooling rate) and Zagami (*e.g.*, pyroxene and plagioclase compositions). The crystallization sequence of pyroxenes in Dhofar 019 may suggest crystallization of lithology A of EETA79001 (also Dar al Gani and Sayh al Uhaymir shergottites) followed by Zagami from the same magma. A magma mixing process involving both magnesian and ferroan olivine xenocrysts might cause the petrogenesis of Dhofar 019. Alternatively, ferroan olivines could be phenocrysts that crystallized with the groundmass pyroxenes and plagioclase. At any rate, Dhofar 019 appears to have experienced a complex history. The chemical composition of Dhofar 019 olivines are distinct from any other olivines in both basaltic and lherzolithic shergottites. The preservation of chemical zoning in olivine and homogeneous olivines with variable compositions suggest rapid crystallization of Dhofar 019 near the martian surface (burial depth: ~5 m), possibly in a lava flow.

Acknowledgments

We thank Drs. T. J. McCoy, G. A. McKay and an anonymous reviewer for their constructive reviews of the manuscript. We are also indebted to Mr. O. Tachikawa and H. Yoshida for technical assistance during electron beam analyses. The electron microscopy was performed in the Electron Microbeam Analysis Facility for mineralogy at Department of Earth and Planetary Science, University of Tokyo. This work was

supported in part by the Grant-in-Aid for Encouragement of Young Scientists by the Japanese Ministry of Education, Science and Culture (No. 12740297).

References

- Barrat, J.A., Blichert-Toft, J., Nesbitt, R.W. and Keller, F. (2001): Bulk chemistry of Saharan shergottite Dar al Gani 476. *Meteorit. Planet. Sci.*, **36**, 23–30.
- Barrat, J.A., Jambon, A., Bohn, M., Gillet, Ph., Sautter, V., Gopel, C., Lesourd, M. and Keller, F. (2002): The picritic shergottite North West Africa 1068 (NWA 1068 or “Louise Michel”). *Lunar and Planetary Science XXXIII*. Houston, Lunar Planet. Inst., Abstract #1538 (CD-ROM).
- Bartoschewitz, R. and Ackermann, D. (2001): Dar al Gani 876, a further fragment of the DaG-Shergottite. *Meteorit. Planet. Sci.*, **36**, Suppl., A15.
- Borg, L.E., Nyquist, L.E., Wiesmann, H. and Reese, Y. (2001a): Rubidium-strontium and samarium-neodymium isotopic systematics of the lherzolithic shergottites ALH77005 and LEW88516: Constraints on the petrogenesis of martian meteorites. *Meteorit. Planet. Sci.*, **36**, Suppl., A24.
- Borg, L.E., Nyquist, L.E., Wiesmann, H., Reese, Y. and Papike, J.J. (2001b): Sr-Nd isotopic systematics of martian meteorite DaG 476. *Lunar and Planetary Science XXXII*. Houston, Lunar Planet. Inst., Abstract #1036 (CD-ROM).
- Buening, D.K. and Buseck, P.R. (1973): Fe-Mg lattice diffusion in olivine. *J. Geophys. Res.*, **78**, 6852–6862.
- Chakraborty, S. (1997): Rate and mechanism of Fe-Mg interdiffusion in olivine at 980°–1300°C. *J. Geophys. Res.*, **102**, 12317–12331.
- Crozaz, G. and Wadhwa, M. (2001): The terrestrial alteration of Saharan shergottites Dar al Gani 476 and 489: A case study of weathering in a hot desert environment. *Geochim. Cosmochim. Acta*, **65**, 971–977.
- Folco, L., Franchi, I.A., D’Orazio, M., Rocchi, S. and Schultz, L. (2000): A new martian meteorite from the Sahara: The shergottite Dar al Gani 489. *Meteorit. Planet. Sci.*, **35**, 827–839.
- Folco, L. and Franchi, I. A. (2000): Dar al Gani 670 shergottite: A new fragment of the Dar al Gani 476/489 martian meteorite. *Meteorit. Planet. Sci.*, **35**, Suppl., A54.
- Gooding, J.L., Wentworth, S.J. and Zolensky, M.E. (1988): Calcium carbonate and sulfate of possible extraterrestrial origin in the EETA 79001 meteorite. *Geochim. Cosmochim. Acta*, **52**, 909–915.
- Grossman, J.N. (2000): The Meteoritical Bulletin, No. 84, 2000 August. *Meteorit. Planet. Sci.*, **35**, Suppl., A199–A225.
- Grossman, J.N. and Zipfel, J. (2001): The Meteoritical Bulletin, No. 85, 2001 September. *Meteorit. Planet. Sci.*, **36**, Suppl., A293–A322.
- Harvey, R.P., Wadhwa, M., McSween, H.Y., Jr. and Crozaz, G. (1993): Petrography, mineral chemistry and petrogenesis of Antarctic shergottite LEW 88516. *Geochim. Cosmochim. Acta*, **57**, 4769–4783.
- Hofmann, B.A., Gnos, E., Hauser, M., Moser, L., Al Kathiri, A. and Franchi, I. A. (2001): The 2001 Omani-Swiss meteorite search campaign and recovery of shergottite Sayh al Uhaymir 094. *Meteorit. Planet. Sci.*, **36**, Suppl., A82.
- Ikeda, Y. (1994): Petrography and petrology of the ALH-77005 shergottite. *Proc. NIPR Symp. Antarct. Meteorites*, **7**, 9–29.
- Lentz, R.C.F. and McSween, H.Y., Jr. (2001): Small olivines in Dhofar 019: Indicators of a complex petrogenesis. *Meteorit. Planet. Sci.*, **36**, Suppl., A111.
- Lentz, R.C.F., McSween, H.Y., Jr., Nazarov, M.A. and Taylor, L.A. (2001): A textural consideration of Dhofar 019 with comparisons to other basaltic shergottites. *Lunar and Planetary Science XXXII*. Houston, Lunar Planet. Inst., Abstract #1742 (CD-ROM).
- McCoy, T.J., Taylor, G.J. and Keil, K. (1992): Zagami: Product of a two-stage magmatic history. *Geochim. Cosmochim. Acta*, **56**, 3571–3582.
- McCoy, T.J., Wadhwa, M. and Keil, K. (1999): New lithologies in the Zagami meteorite: Evidence for fractional crystallization of a single magma unit on Mars. *Geochim. Cosmochim. Acta*, **63**, 1249–1262.
- McKay, G.A., Miyamoto, M., Mikouchi, T. and Ogawa, T. (1998): The cooling history of the LEW 86010 angrite as inferred from kirschsteinite lamellae in olivine. *Meteorit. Planet. Sci.*, **33**, 977–983.
- McSween, H.Y., Jr. (1994): What we have learned about Mars from SNC meteorites. *Meteoritics*, **29**, 757–

779.

- McSween, H.Y., Jr. and Jarosewich, E. (1983): Petrogenesis of the Elephant Moraine A 79001 meteorite: Multiple magma pulses on the shergottite parent body. *Geochim. Cosmochim. Acta*, **47**, 1501–1513.
- Mikouchi, T. and Miyamoto, M. (2000): Martian lherzolitic meteorites Allan Hills 77005, Lewis Cliff 88516 and Yamato-793605: Major and minor element zoning in pyroxene and plagioclase glass. *Antarct. Meteorite Res.*, **13**, 256–269.
- Mikouchi, T., Miyamoto, M. and McKay, G. (1998): Mineralogy of Antarctic basaltic shergottite Queen Alexandra Range 94201: Similarities to Elephant Moraine A 79001 (Lithology B) martian meteorite. *Meteorit. Planet. Sci.*, **33**, 181–189.
- Mikouchi, T., Miyamoto, M. and McKay, G. (1999): The role of undercooling in producing igneous zoning trends in pyroxenes and maskelynites among basaltic Martian meteorites. *Earth Planet. Sci. Lett.*, **173**, 235–256.
- Mikouchi, T., Miyamoto, M. and McKay, G. (2001): Mineralogy and petrology of the Dar al Gani 476 martian meteorite: Implications for its cooling history and relationship to other shergottites. *Meteorit. Planet. Sci.*, **36**, 531–548.
- Misener, D.J. (1974): Cation diffusion in olivine to 1400°C and 35 kbar. *Geochemical Transport and Kinetics*, ed. by A.W. Hoffmann *et al.* Washington D.C., Carnegie Inst. of Washington, 117–129.
- Mittlefehldt, D.W., Lindstrom, D.J., Lindstrom, M.M. and Martinez, R.R. (1999): An impact melt origin for lithology A of martian meteorite EETA 79001. *Meteorit. Planet. Sci.*, **34**, 357–367.
- Miyamoto, M. and Mikouchi, T. (1998): Evaluation of diffusion coefficients of Fe-Mg and Ca in olivine. *Mineral. J.*, **20**, 9–18.
- Miyamoto, M. and Mikouchi, T. (2001): Evaluation of the iron-magnesium diffusion coefficient in olivine. *Meteorit. Planet. Sci.*, **35**, Suppl., A138.
- Nishiizumi, K., Caffee, M.W., Jull, A.J.T. and Klandrud, S.E. (2001): Exposure histories of shergottites Dar al Gani 476/489/670/735 and Sayh al Uhaymir 005. *Lunar and Planetary Science XXXII*. Houston, Lunar Planet. Inst., Abstract #2117 (CD-ROM).
- Nishiizumi, K., Okazaki, R., Park, J., Nagao, K., Masarik, J. and Finkel, R.C. (2002): Exposure and terrestrial histories of Dhofar 019 martian meteorite. *Lunar and Planetary Science XXXIII*. Houston, Lunar Planet. Inst., Abstract #1366 (CD-ROM).
- Ostertag, R., Amthauer, G., Rager, H. and McSween, H. Y. (1984): Fe³⁺ in shocked olivine crystals of the ALHA 77005 meteorite. *Earth Planet. Sci. Lett.*, **67**, 162–166.
- Steele, I.M. and Smith, J.V. (1982): Petrography and mineralogy of two basalts and olivine-pyroxene-spinel fragments in achondrite EETA 79001. *Proc. Lunar Planet. Sci. Conf.*, 13th, Pt. 1, A375–A384 (*J. Geophys. Res.*, **87** Suppl.).
- Taylor, L.A., Nazarov, M.A., Ivanova, M.A., Patchen, A., Clayton, R.N. and Mayeda, T.K. (2000): Petrology of the Dhofar 019 shergottite. *Meteorit. Planet. Sci.*, **35**, Suppl., A155.
- Treiman, A. H., McKay, G.A., Bogard, D.D., Mittlefehldt, D.W., Wang, M.-S., Keller, L., Lipshutz, M.E., Lindstrom, M.M. and Garrison, D. (1994): Comparison of the LEW 88516 and ALHA 77005 martian meteorites: Similar but distinct. *Meteoritics*, **29**, 581–592.
- Wadhwa, M., Lentz, R.C.F., McSween, H.Y. and Crozaz, G., Jr. (2001): A petrologic and trace element study of Dar al Gani 476 and Dar al Gani 489: Twin meteorites with affinities to basaltic and lherzolitic shergottites. *Meteorit. Planet. Sci.*, **36**, 195–208.
- Zipfel, J. (2000): Sayh Al Uhaymir 005/008 and its relationship to Dar al Gani 476/489. *Meteorit. Planet. Sci.*, **35**, Suppl., A178.
- Zipfel, J., Scherer, P., Spettel, B., Dreibus, G. and Schultz, L. (2000): Petrology and chemistry of the new shergottite Dar al Gani 476. *Meteorit. Planet. Sci.*, **35**, 95–106.

(Received December 3, 2001; Revised manuscript accepted January 29, 2002)